

# 1 Materials and Methods

## 2 1.1 Geological unit information

All information used in this analysis is available freely through Macrostrat  
4 [macrostrat.org](http://macrostrat.org) and the Paleobiological Database PBDB [paleobiodb.org](http://paleobiodb.org).  
For this analysis, we used direct API calls to pull data from the relational  
6 databases underpinning both Macrostrat and the PBDB (Peters and McClennen,  
2015, Peters et al., 2018); this means that our analyses are inherently dynamic  
8 and can be instantly updated as these databases continue to grow.

Macrostrat geological units that have some amount of their sediments within  
10 the Ordovician or Silurian; this requires two API calls to Macrostrat, one for  
each of the periods (e.g.  
12 [macrostrat.org/api/v2/units?interval\\_name=Ordovician](http://macrostrat.org/api/v2/units?interval_name=Ordovician)). These data  
frames were merged using a left-join with geological unit identification code  
14 (`unit_id`) as the key value which prevents double counting of geologic units that  
range through both periods.

16 The key value of geological unit metadata associated with this data frame are  
the unique identifiers for each geological unit. These values can be used as the  
18 key value for linking these geological units to the fossils found within those  
units (e.g. [macrostrat.org/api/v2/fossils?unit\\_id=...](http://macrostrat.org/api/v2/fossils?unit_id=...)). This aspect of  
20 the Macrostrat database includes information on the count of Paleobiology  
Database collections drawn from that unit, the count of unique fossils listed in  
22 the Paleobiology Database associated with that unit, the unique taxonomic  
identifiers for each of those fossils, and the unique identifiers for each of the  
24 collections drawn from that unit (`cltn_id`). This final value acts as the foreign  
key for extracting fossil occurrence and taxonomic information from the

26 Paleobiology Database.

A final API call is made, this time to Paleobiology Database, using the  
28 collection id foreign key from Macrostrat (e.g.  
`paleobiodb.org/data1.2/occs/list.txt?coll_id=...`); this API call was  
30 technically done as two calls and the resulting union of those data frames is a  
data frame with all the metadata for all of the fossil occurrences in collections  
32 drawn from geological units from the Ordovician and Silurian present in  
Macrostrat.

34 For a more explicit and exacting description of the data gathering and  
preparing process, please see the `./R/download_scrap.r` and `/R/prepare_data.r`  
36 scripts from the project repository [https://github.com/psmits/not\\_fossil](https://github.com/psmits/not_fossil).

The above series of API calls produces three data frames: Macrostrat geological  
38 units and their metadata, fossil counts and collection information for those  
Macrostrat geological units, and the unique fossils present in these units and  
40 their metadata from the Paleobiology database.

An interesting feature of Macrostrat geologic units is that they are ordered  
42 according to the underlying continuous-time age model (Peters et al., 2018).  
This age model increases the overall resolution of the geological record.  
44 Unfortunately the fossil collection information for each unit does not include  
within-unit superposition data; this means that the diversity within a geologic  
46 unit cannot be tracked over the duration of the unit but only as a function of  
the complete unit. Because of this, the most precise unit of our analysis is the  
48 geologic unit. Specifically, we assign each geologic units to a single temporal  
bins based on which bin contained their midpoint. Macrostrat provides a top  
50 and bottom age and by averaging those we get the midpoint age. In total, we  
divided the data into 20 uniform-duration discrete time intervals.

52 The geological unit metadata values that are relevant to this analysis include  
areal extent of the unit (positive, real values), maximum unit thickness  
54 (positive, real values), average paleo latitudinal position (real values), and the  
lithological description of the unit. Lithology is expressed as one or more  
56 natural language statements (e.g. siliclastic sedimentary) and the percentage of  
the unit associated with that lithology.

58 Lithological description, being made of natural language statements, requires  
some standardization and simplification to make it amenable to analysis.  
60 Ultimately, we described lithology as some combination of fine siliciclastics,  
coarse siliciclastics, dolomitic carbonates, and non-dolomitic carbonates. The  
62 multi-step process to reduce the original natural language descriptions is  
detailed here, but for the complete and explicit process the `strict.lithology`  
64 function in `./R/rock_mung.r` script file from the project repository  
[https://github.com/psmits/not\\_fossil](https://github.com/psmits/not_fossil).

66 First, units that have at least one description including the words igneous,  
volcanic, metamorphic, chemical, anhydrite, evaporite, or halite were removed  
68 prior to analysis. After this step, descriptive terms were unified so that the  
natural language descriptions are easier match together (e.g. green and greenish  
70 become green, mudstone and mud become mudstone). Next, some additional  
words were removed from descriptions for either being too general or too  
72 specific (e.g. sedimentary, dark, etc.). Each of these choices are inherently  
arbitrary means of simplifying text, but these ultimately have little to no effect  
74 the final descriptions because our final step is extremely strict.

This final step in assigning the final lithological descriptions to simpler values  
76 that are amenable to analysis. Descriptions were classified as “fine siliciclastics”  
were those containing at least one of the terms siltstone, claystone, mudstone,  
78 shale, and argillite. In contrast, descriptions were classified as “coarse

siliciclastics” if they were a siliciclastic lithology that did not include one of the  
80 terms keyed to “fine siliciclastics”. Descriptions were classified as “dolomitic  
carbonates” if those lithological descriptions contained the word “dolomite”.  
82 Finally, non-dolomitic carbonates were all other carbonate lithologies.

Prior to analysis, real values were log transformed by subtracting the mean  
84 value from all observations then dividing by twice the standard deviation of the  
observations. Similarly, positive real valued covariates were log-plus-one  
86 transformed and then rescaled in a similar manner. Rescaling the covariates has  
multiple advantages: 1) regression coefficients now describe the expected change  
88 in unit diversity per change in standard deviation of covariate, and 2) regression  
coefficients are comparable across covariates because they are all on the same  
90 scale (the expected standard deviation of a binary variable is 0.5) (Gelman and  
Hill, 2006).

92 In contrast to the other covariations, compositional covariates are constrained  
to sum to 1 which creates degrees-of-freedom issues when trying to model their  
94 possible effects as including these covariates without appropriate transformation  
creates two or more nonidentifiable parameters. To that end, the composition  
96 variables were isometric log-ratio transformed (ilr) (Egozcue et al., 2003) which  
reduces the total number of variables to one less than original as composition is  
98 defined in relation to a baseline (percent non-dolomitic carbonates).

Unfortunately, the scale and interpretations of the associated regression  
100 coefficients are different from the other covariates, making direct comparison  
tricky. The ilr transformation was done using the `compositions` package for  
102 R (van den Boogaart et al., 2014).

The fossil occurrence and diversity for each of the geological units was  
104 determined for each of the following taxonomic groups: Anthozoa, Brachiopoda,  
Bivalvia, Cephalopoda, Gastropoda, and Trilobita. Fossil membership was

106 determined based on the metadata for phylum or class from the Paleobiology  
database. We fit our model separately to each of these datasets.

## 108 **1.2 Modeling of the fossil diversity found in a geologic units**

110 All geologic units we're analyzing have at least one species occurrence  
associated with it; this explicit observation restriction means that instead of a  
112 full distribution of counts from 0 to positive infinity, we instead have a  
truncated distribution ranging from 1 to positive infinity.

114 A natural statistical distribution for discrete data is the Poisson distribution.  
The Poisson distribution makes strong assumptions about the mean-variance  
116 relationship of the data which is rarely found in life as data frequently has much  
larger variance in counts than the mean count; this variance is described as  
118 overdispersion as the data has a greater scale than expected from a Poisson  
distribution (Gelman and Hill, 2006, Gelman et al., 2014). TO model this  
120 potential overdispersion in the data, we opted for using the Negative Binomial  
distribution instead of the Poisson. The Negative Binomial distribution can be  
122 derived as a mixture a Gamma and a Poisson distribution where the Gamma  
accounts for increased variance.

124 The Negative Binomial distribution parameterized in terms of of mean or  
expected count  $\mu$  and a description of the dispersion of the data  $\phi$  is formulated  
126 as:

$$\text{Negative Binomial}(y|\mu, \phi) = \binom{y + \phi - 1}{y} \frac{\mu}{\mu + \phi} \frac{\mu}{\mu + \phi} \frac{\phi}{\mu + \phi}^{\phi} . \quad (1)$$

We chose this parameterization of the Negative Binomial distribution because it  
128 has one of the simplest interpretations; the mean  $\mu$  is the expected taxonomic

diversity of a given geologic unit, and the amount of overdispersion in counts is  
130 equal to the inverse of  $\phi$  scaled by the square of the mean  $\mu$ . Our  
hierarchical/multi-level model can be characterized as a type of GLMM with  
132 varying-intercept and varying-slopes where the assumed data distribution is a  
zero-truncated Negative Binomial distribution and our regression uses a log-link  
134 function. For a more detailed description of the Negative Binomial distribution  
and its use in count regression please see Gelman and Hill (2006).

136 The effects of the unit covariates are expressed as the regression coefficients  $\beta$   
which were allowed to vary over time  $t$ . The temporal structure of the covariates  
138 was modeled as a random walk prior on the matrix of time-level means  $\gamma$ ; a  
random-walk prior is a simple way of constraining the estimates for  $\beta_t$  given the  
140 estimate of  $\beta_{t-1}$ . Additionally, the scale parameters  $\sigma$  for each of the  $K$   
coefficients are related to the rate of change over time; a low value of  $\sigma_k$   
142 corresponds to little between time variance in the effect of that covariate on  
diversity while a large value of  $\sigma_k$  indicates that the effect of that covariate is  
144 inconsistent through time. The values  $I$  and  $S$  are hyperprior values that we  
specified based on our prior expectations of average unit diversity (Table 1).

$$\begin{aligned}
\mu_i &= \exp(X_i \beta_{t[i]}) \\
\beta_t &\sim \text{MVN}(\gamma_t, \Sigma) \\
\gamma_{t,k} &\sim \begin{cases} \mathcal{N}(I, S) & \text{if } t = 1 \\ \mathcal{N}(0, 1) & \text{if } t = 1, k \neq 1 \\ \mathcal{N}(\gamma_{t-1,k}, \sigma_k) & \text{if } t > 1, k \neq 1 \end{cases} \quad (2) \\
\sigma_k &\sim \mathcal{N}^+(1) \\
\frac{1}{\phi} &\sim \mathcal{N}^+(1).
\end{aligned}$$

146 The additional covariance between variation in the regression coefficients  $\beta$  over  
time that not accounted for by the random-walk prior on  $\gamma$  are modeled by the  
148 unknown/estimated covariance matrix  $\Sigma$ . In order to improve sampling  
performance and choice of priors, the covariance matrix was decomposed into a  
150 vector of scales  $\tau$  and a correlation matrix  $\Omega$  as recommended by the Stan  
manual (Team, 2017). Their associated priors are as follows:

$$\begin{aligned}\Sigma &= \text{diag}(\tau)\Omega\text{diag}\tau \\ \Omega &\sim \text{LKJ}(1) \\ \tau &\sim \mathcal{N}^+(1).\end{aligned}\tag{3}$$

152 The correlation matrix  $\Omega$  was given a LKJ distribution prior based on  
recommendations in Stan manual. This distribution has a single parameter  
154 where values close to 0 correspond to a uniform distribution across all possible  
correlation matrices, and as values increase this distribution convergences on an  
156 identity matrix. This weakly-informative prior nudges our estimates towards a  
result of no correlation between covariate effects over time though is not  
158 sufficiently strong enough to prevent us inferring a possible correlation if there  
is there is enough evidence.

160 Unless otherwise noted, all prior choices reflect our decision to use  
weakly-informative regularizing priors. Additionally, because all covariates are  
162 on approximately unit scale and we do not expect any of our regression  
coefficients to have magnitude greater than 2, more diffuse priors would serve no  
164 purpose and are unnecessary. Additionally, more diffuse priors would not reflect  
our actual expectations regarding the magnitude of covariate effects. Finally,  
166 the regularizing property of priors helps constrain our results such that we do  
not obtain spurious estimates of the covariate effects (Gelman et al., 2014,

Taxonomic group	Intercept prior mean $I$	Intercept prior scale $S$	Dispersion scale $H$
Anthozoa	1	2	3
Brachiopoda	2	2	5
Bivalvia	1	2	3
Cephalopoda	2	2	5
Gastropoda	2	2	5
Trilobita	2	2	5

Table 1: Key prior choices for each of the taxonomic groups included in this analysis. Prior choice reflects our expectations of the average diversity of that group in a geologic unit.

2008); see also [http://mc-stan.org/users/documentation/case-studies/weakly\\_informative\\_shapes.html](http://mc-stan.org/users/documentation/case-studies/weakly_informative_shapes.html)

In total, the complete model is as follows

$$\begin{aligned}
y &\sim \text{Negative Binomial}(\mu, \phi)T[1,] \\
\mu_i &= \exp(X_i \beta_{t[i]}) \\
\beta_t &\sim \text{MVN}(\gamma_t, \Sigma) \\
\gamma_{t,k} &\sim \begin{cases} \mathcal{N}(I, S) & \text{if } t = 1 \\ \mathcal{N}(0, 1) & \text{if } t = 1, k \neq 1 \\ \mathcal{N}(\gamma_{t-1,k}, \sigma_k) & \text{if } t > 1, k \neq 1 \end{cases} \\
\frac{1}{\phi} &\sim \mathcal{N}^+(1). \\
\sigma_k &\sim \mathcal{N}^+(1) \\
\Sigma &= \text{diag}(\tau) \Omega \text{diag} \tau \\
\Omega &\sim \text{LKJ}(2) \\
\tau &\sim \mathcal{N}^+(1).
\end{aligned} \tag{4}$$

As stated earlier, for all taxonomic groups the intercept term is an estimate of



the expected (log) geologic unit diversity for a geologic unit with mean thickness, area, latitude, and a purely non-dolomitic carbonate lithology. The effects of thickness, area, and latitude correspond to the expected change in (log) geologic unit diversity per change of the covariate value in standard deviations. The effects of dolomite, fine and coarse siliciclastic correspond to the change associated with unit change to the logration representing the compositional part of interest (Hron et al., 2012).

### 1.2.1 Implementing model in Stan

The joint posterior was approximated using a Markov-chain Monte Carlo routine that is a variant of Hamiltonian Monte Carlo called the No-U-Turn Sampler as implemented in the probabilistic programming language Stan (Carpenter et al., 2017). The posterior distribution was approximated from four parallel chains run for 40,000 steps, split half warm-up and half sampling and thinned to every 20th sample for a total of 4000 posterior samples. Chain convergence was assessed via the scale reduction factor  $\hat{R}$  where values close to 1 ( $\hat{R} < 1.1$ ) indicate approximate convergence. Convergence means that the chains are approximately stationary and the samples are well mixed (Gelman et al., 2014). After the model was fit to the data, 100 datasets were simulated from the posterior predictive distribution of the model. These simulations were used to test for adequacy of model fit as described below.

Hierarchical models can have very complex posterior geometries which make full exploration of the log-posterior surface difficult Stan manual (Team, 2017). The two strategies for overcoming sampling pathologies associated with sampling an extremely convoluted log-posterior surface are a non-centered parameterization of the normal distribution used to describe hierarchical structure in the model, as well as adjusting some the key parameters governing Stan’s sampling

198 adaptation phase.

Non-centered parameterization help mitigate divergences because this separates  
200 the location from the scale, thus “opening” up the log-posterior surface. The  
cost of this reparameterization is the addition of one parameter per regression  
202 coefficient, though this parameter has good sampling behavior is relatively  
constrained by a regularizing prior. For the details of what that means and how  
204 this change in parameterization improves sampling please see Betancourt and  
Girolami (2013) and the Stan manual (Team, 2017).

206 The above model specifications (Eq. 4) were modified as follows:

$$\begin{aligned}\beta_t &= \gamma_t + z\Sigma \\ \gamma'_{t,1} &\sim \mathcal{N}(I, S) \quad \text{if } t = 1 \\ \gamma'_{t,-} &\sim \mathcal{N}(0, 1) \quad \text{if } t = 1 \text{ and } k > 1 \\ \gamma'_{t,-} &\sim \mathcal{N}(0, 1) \quad \text{if } t > 1 \\ z &\sim \mathcal{N}(0, 1)\end{aligned}\tag{5}$$

We used five different diagnostic criteria to determine if our chains were well  
208 mixed and if our posterior estimates were based on unbiased samples: the scale  
reduction factor  $\hat{R}$  (target value of  $<1.1$ ), effective number of samples (eff;  
210 target value of  $\text{eff}/\text{steps} < 0.0001$ ), if any samples saturated the specified  
maximum trajectory length for avoiding infinite loops (treedepth; target value  
212 of 0 samples), presence of divergent samples which indicate pathological  
sampling in some neighborhoods of the log-posterior (divergences; target value  
214 of 0 samples), and the energy Bayesian Fraction of Missing Information  
(E-BFMI; target value  $>0.2$ ). For a further explanation of these diagnostic  
216 criteria see Stan manual (Team, 2017).

Taxonomic group	chain steps (half warm-up, half sample)	thinning	adapt delta	max tree dep
Anthozoa				
Bivalvia				
Brachiopoda				
Gastropoda				
Trilobita				
(Bivalvia + Gastropoda)				

Table 2: Settings for the Stan sampler for estimating model posterior densities.

Stan’s adaptation phase can be adjusted to help overcome issues resulting from  
 218 extremely high curvature of the log-posterior. Ultimately, estimation of the joint  
 posterior distributions for each of the taxonomic datasets required different  
 220 settings for the number of steps for each chain as well as multiple model  
 adaptation parameters (Table 2).

222 Model adequacy was evaluated using a series of posterior predictive checks. The  
 concept of model adequacy is that if our model is an adequate descriptor of the  
 224 observed data, then data simulated from the posterior predictive distribution  
 should be similar to the observed given the same covariates, etc. (Gelman et al.,  
 226 2014). Posterior predictive checks can take many forms but the basic idea is to  
 compare some property of the empirical data to that property estimated from  
 228 each of the simulated datasets. For each check, the value of a test statistic from  
 the data is compared to a distribution of that test statistic estimated from  
 230 datasets simulated from the posterior. Model adequacy is indicated by our  
 simulated values being approximately equal to the observed values.

232 We used a variety of posterior predictive checks to assess the quality of model’s  
 fit to each of the different datasets. The goal of using this many and variety of  
 234 checks is understand the quality and nature of model fit. For example, our  
 model may have good fit to many aspects of the data but “fail” one or more  
 236 checks, highlighting potential differences between our model and the data  
 generating process thus promoting further study (Gelman and Hill, 2006,

238 Gelman et al., 2014). For example if there was obvious divergence between our  
models and the data we would not have confidence in any downstream analyses  
240 or hypothesis tests, and we would instead question how or why our model fails  
and possibly improve our model to better reflect important unmodeled variance.

242 The checks used here are comparisons of the overall mean unit diversity, the  
overall standard deviation of unit diversity, the mean unit diversity for each  
244 time step, and the standard deviation of unit diversity for each time step to  
those test statistics from 1000 posterior predictive datasets. Most of these  
246 posterior predictive checks were done using the `bayesplot` package for R  
(Gabry and Mahr, 2018).

## 248 **2 Results**

### **2.1 Posterior predictive results**

250 Overall, the expected taxonomic diversity of geological units for each taxonomic  
group is adequately described by the fitted models, where adequacy means that  
252 the posterior predictive distribution of our models resemble the empirical data.  
While there are aspects of misfit when considering their entire distribution, the  
254 aspects of the distribution which are critical to our analysis are well fit by our  
models.

256 A point comparison between the observed mean geologic unit diversities and the  
posterior predictive distributions for each taxonomic group indicate that our  
258 fitted models are able to recapitulate this aspect of the observed data (Fig. 1).  
This result is reassuring because our model is specifically a model of expected  
260 geologic unit diversity, and a good fit to mean diversity means our model fits  
are at least capturing this basic aspect of the data.

262 Comparison of the observed standard deviation estimates for each of the  
taxonomic datasets to the posterior predictive distributions of our model fits  
264 show that our model is slightly over estimating the scale of our data, though not  
to a necessarily concerning degree (Fig. 2). Count data can frequently be over  
266 dispersed and have a standard deviation to mean ratio greater than 1; this  
reality is the reason we chose to use a truncated Negative-Binomial as opposed  
268 to a Poisson distribution because the addition of a second parameter allows us  
to model this overdispersion (Gelman and Hill, 2006, Gelman et al., 2014).

270 While our model is not too different from the data, there is room for  
improvement in modeling the actual dispersion of geologic unit diversity.

272 Comparisons of the empirical probability density functions for each of the

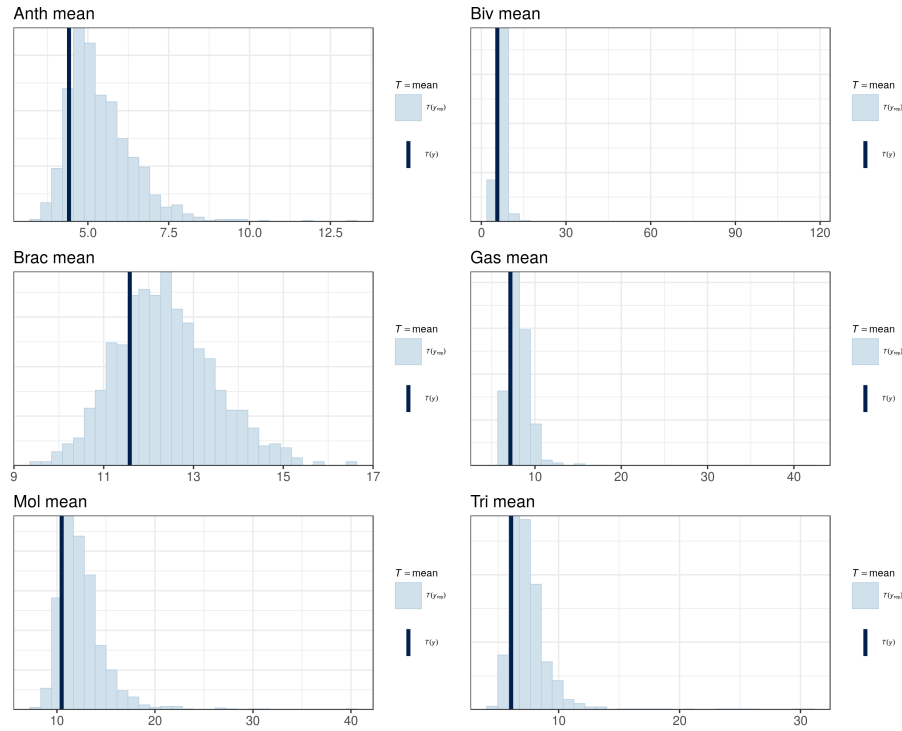


Figure 1: Posterior predictive results comparing the observed mean diversity of a geological unit for each of the studied taxonomic groups to a distribution of 1000 estimates from datasets simulated from the posterior predictive distribution of our models. Model adequacy is determined by how similar the posterior predictive distribution is to the observed value. In all cases, our models appear able to reproduce to observed means.

taxonomic groups to the posterior predictive distribution of density functions  
 274 generated by our model fits indicate that our model is very capable of  
 recapitulating the observed data for nearly its entire range (Fig. 3). There are,  
 276 however, minor but noticable differences between the posterior predictive  
 distribution and the empirical data. For example, the posterior predictive  
 278 distribution for Anthozoa slightly underestimates the number of units with  
 diversity approximately 8. A similar underestimate is observable when  
 280 comparing the posterior predictive distribution to the empirical data at unit  
 diversity of approximately 11, and Brachiopoda at unit diversity of

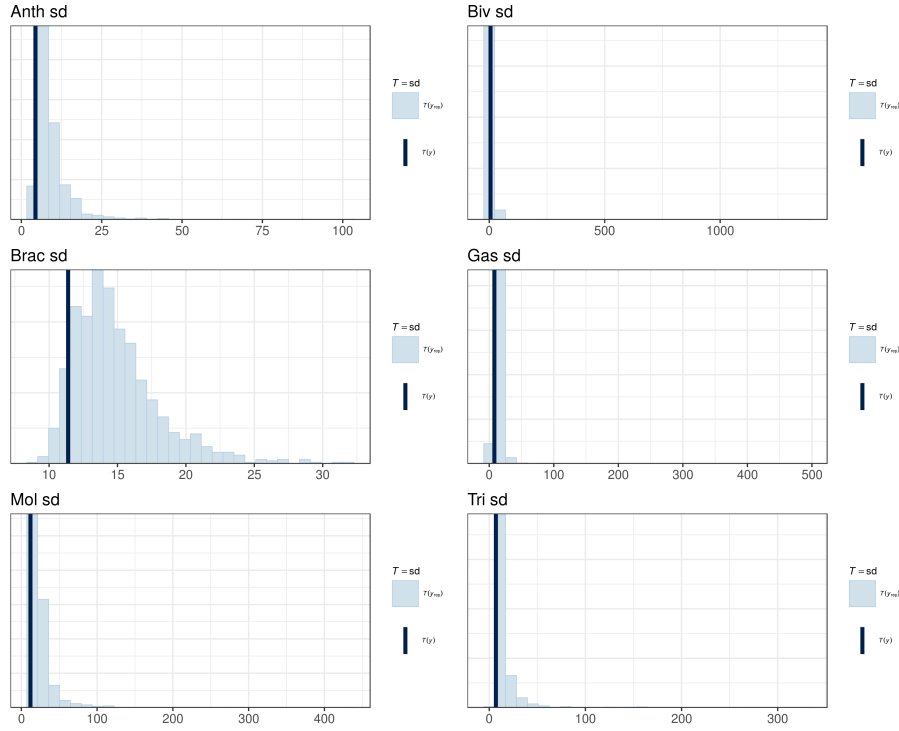


Figure 2: Posterior predictive results comparing the observed standard deviation diversity of a geological unit for each of the studied taxonomic groups to a distribution of 1000 estimates from datasets simulated from the posterior predictive distribution of our models. Model adequacy is determined by how similar the posterior predictive distribution is to the observed value. In all cases, our models appear able to reproduce to observed standard deviations.

approximately 11. However, the posterior predictive distributions of our models fit the data well in nearly all cases, indicating that our model is potentially capturing some aspects of the data generating process.

## 2.2 Estimated versus observed unit diversity

Comparison between observed unit diversity over time and our models' estimates of mean unit diversity for those time steps reveals broad congruence (Fig. 4). At no point does our model have a spurious or unrealistic estimate of

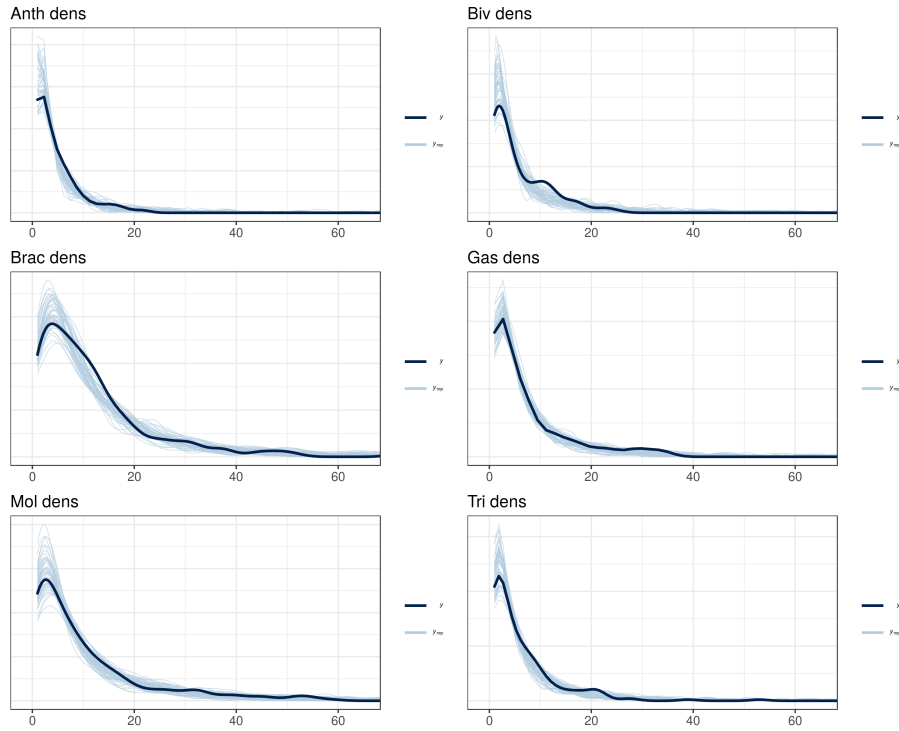


Figure 3: Posterior predictive results comparing the empirical probability density of a geological unit for each of the studied taxonomic groups to a distribution of 1000 probability densities from datasets simulated from the posterior predictive distribution of our models. Model adequacy is determined by how similar the posterior predictive distribution is to the observed value. In all cases, our models appear able to almost reproduce to observed ecdf-s.

mean geologic unit taxonomic diversity. This congruence gives us confidence in  
 290 estimating the probability of the Hirnantian (1) having lower average unit  
 diversity than the times directly before and after, and (2) having lower average  
 292 unit diversity than the average unit diversity of the late Ordovician and the  
 Silurian.

294 We tested the probability that geologic units during the Hirnantian have lower  
 expected unit diversity than the times immediately before and after by testing  
 296 all adjacent time bins (Fig. 5). For each adjacent time bins, we estimated the



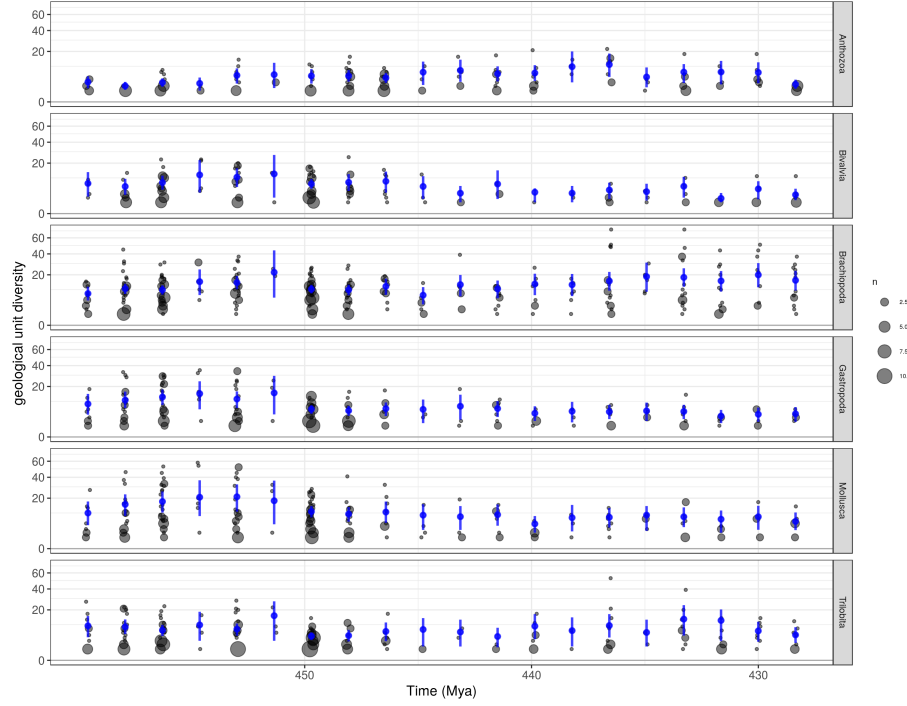


Figure 4: Geological unit diversity through time and the expected diversity (with 80% credible interval) as estimated from our models. Unit diversity is presented as partially transparent points and jittered in the y-axis to improve readability. Point size is proportional to the number of units in that interval that have identical unit diversity. The dashed grey line corresponds to the onset of the Hirnantian geological stage, while the dashed-dotted grey line corresponds to the end of the Ordovician epoch and the start of the Silurian epoch.

probability that the earlier time bin (time  $t$ ) has a greater expected duration  
 298 than the later time bin (time  $t + 1$ ). Our analysis demonstrates that, for most  
 comparisons, the expected unit diversity of Hirnantian time bin is not expected  
 300 with high probability to be different from the time units immediately preceding  
 and following it.

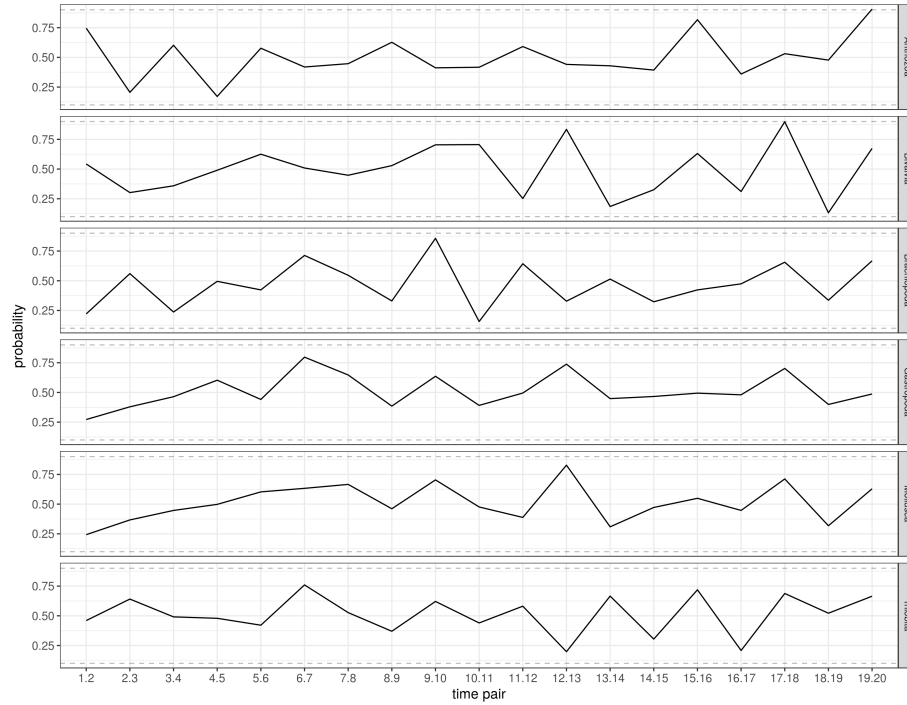


Figure 5: Probability that our estimate of mean unit diversity at time  $t$  is greater than the estimate at time  $t + 1$ . The dashed grey horizontal lines correspond to probability of 0.9 and 0.1; these are the thresholds we chose as indicating if a pair-wise difference is potentially larger (or smaller) than no-difference ( $P = 0.5$ ), and worthy of further inspection.

## 2.3 Effects of geological covariates on estimated diversity

As stated earlier, for all taxonomic groups the intercept term is an estimate of the expected (log) diversity of geologic unit diversity with mean thickness, area, latitude, and a purely non-dolomitic carbonate lithology. The effects of thickness, area, and latitude correspond to the expected change in (log) geologic unit diversity per change of the covariate value in units of standard deviations. The effects of dolomite, fine and coarse siliciclastic correspond to the change associated with unit change to the logratio representing the lithological composition of interest (Hron et al., 2012).

Estimates of covariates effects over time demonstrate a gradual shift in effects

over time and not a sudden shift during the Hirnantian or between the Ordovician and the Silurian (Fig. 6). Interestingly, the covariate that may demonstrate the biggest pattern associated with the Hirnantian is the effect of geologic unit areal extent which appears to decrease in effect for Bivalvia, Gastropoda, and Mollusca.

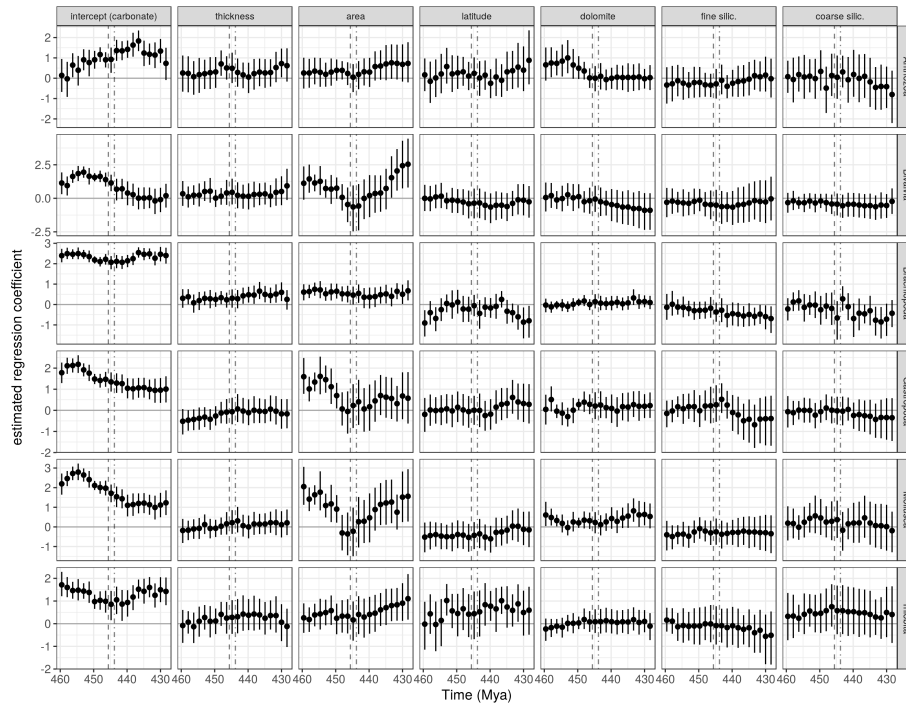


Figure 6: Estimates of all estimated covariate effect time series for each of the analyzed taxonomic groups, including intercept estimates. Points represent mean estimate along with a 80% credible interval. The black horizontal line corresponds to no effect. Points are plotted at the mid-point of the discrete time interval.

316

Similar to our earlier comparison of expected geologic unit diversity, we tested if

any of the covariate effects estimated for one time bin (time  $t$ ) were greater than the estimates from the following time bin (time  $t + 1$ ). We find no strong evidence that the Hirnantian time bin is significantly different from the time

320

bins immediately before and after (Fig. 7). There are very few examples of one  
 322 time bin having significantly different expected unit diversity than the one  
 proceeding it. The intercept of our model fit to the Bivalvia dataset is expected  
 324 to be greater during the second time unit than the third, though this difference  
 is not associated with the Hirnantian time unit and thus is not very relevant to  
 326 the thrust of our analysis. Similarly, we estimated a potentially significant  
 difference the estimated effect of area in Mollusca, where the estimate for the  
 seventh time unit is greater than the estimate for the eighth time unit.

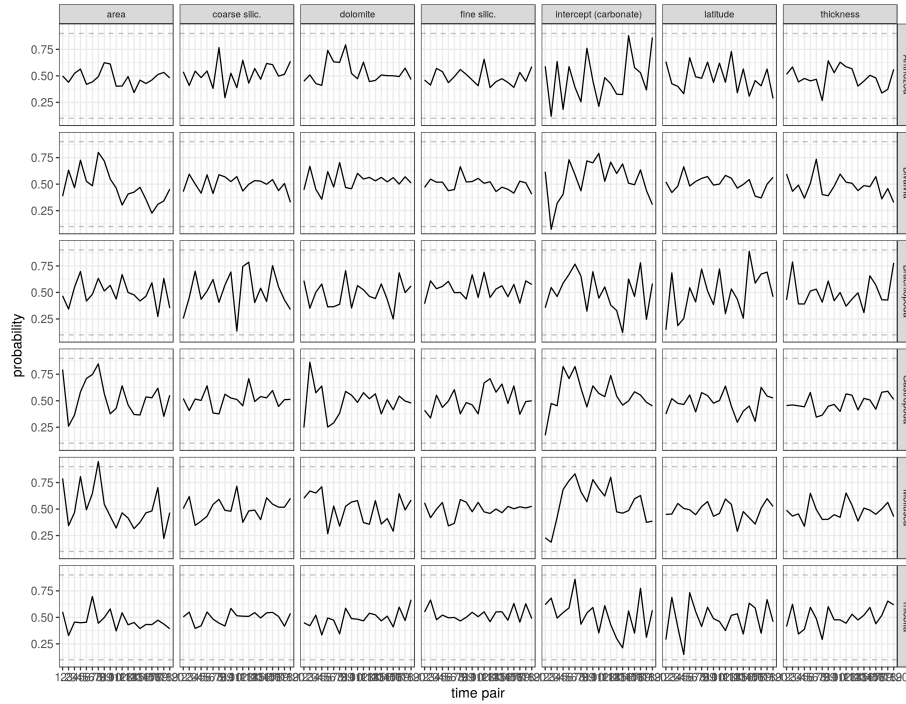


Figure 7: Probability that a parameter estimate at time  $t$  is greater than the estimate at time  $t + 1$ . The dashed grey horizontal lines correspond to probability of 0.9 and 0.1; these are the thresholds we chose as indicating if a pair-wise difference is potentially larger (or smaller) than no-difference ( $P = 0.5$ ), and worthy of further inspection.

328

Of particular interest is if the Hirnantian has a lower expected unit diversity

330 than the average of the Ordovician or Silurian. Additionally, we are interested in  
 if the covariate estimates for the Hirnantian are different than those estimated  
 332 for the rest of the Ordovician or Silurian. Here we calculate the probability that  
 the expected unit diversity of the Hirnantian is less than the averages for the  
 334 Ordovician or Silurian and compare those estimates to the probabilities that the  
 covariate effects are less than the averages for the Ordovician or Silurian (Fig.  
 336 8). We find that in most cases there is no strong evidence (probability  $> 0.9$ ) for  
 the Hirnantian being significantly different from the averages of either the  
 338 Ordovician or the Silurian. However, there is weak evidence (probability  $> 0.75$ )  
 for some differences between the Hirnantian and the Ordovician or Silurian.  
 340 All of the following results are supported with only weak evidence and are thus  
 of interest for future study of lithological and diversity differences associated  
 342 with the Hirnantian.

For Brachiopoda, Gastropoda, and Mollusca the average diversity of geologic  
 344 units in the Ordovician is estimated with weak support to be greater than the  
 expected unit diversity of the Hirnantian. We find weak support for a lower  
 346 effect of dolomite composition on Anthozoan unit diversity during the  
 Hirnantian than the average of the Ordovician. Similarly, we find weak support  
 348 for a lower intercept term and the effect of coarse siliciclastics for Brachiopoda,  
 Gastropoda, Mollusca, and Trilobita in the Hirnantian than the average of the  
 350 Ordovician. The intercept is also the effect of being a purely non-dolomitic  
 carbonate unit. We also find marginal support for the effect of area on unit  
 352 diversity of Bivalvia, Gastropoda, and Mollusca being greater for the average of  
 the Ordovician than those units from the Hirnantian.

354 We do find evidence that Brachiopods are expected to have greater unit  
 diversity during the Silurian than during the Hirnantian. This result is one of  
 356 the strongest support results from this study. Bivalvia and Mollusca intercept

weak evidence expected to be greater in Hirnantian than average Silurian. This  
 358 is also the effect of being a purely non-dolomitic carbonate unit. Bivalvia and  
 Mollusca are estimated to have a lower effect of geologic unit area during the  
 360 Hirnantian than the average of the Silurian. Finally, there is marginal evidence  
 for the intercept estimate for Brachiopoda during the Hirnantian is expected to  
 be lower than the average estimated intercept for the Silurian.

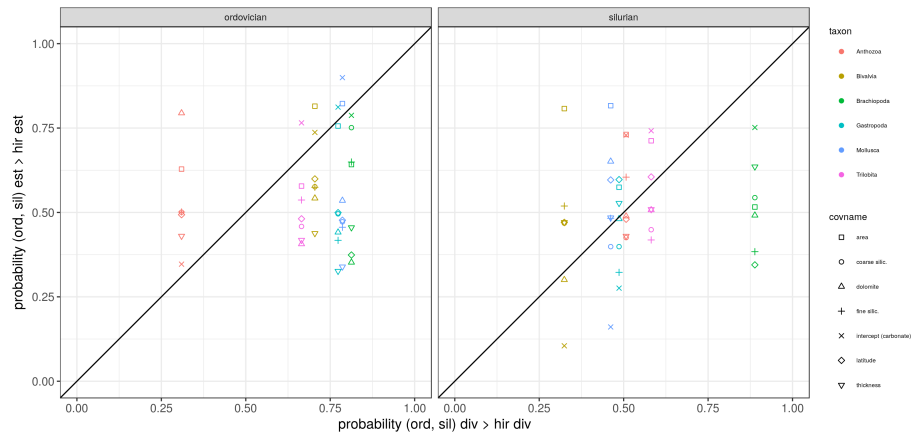


Figure 8: Scatterplot of the estimated probability that geological unit diversity is lower during the Hirnantian than either the Ordovician (left facet) or the Silurian (right facet) vs the estimated probability that a covariate estimate is lower during the Hirnantian than either the Ordovician or the Silurian. For each of the taxonomic groups there is only one estimate for the probability of difference in diversity, but there are six probability estimates for each of the covariate effect parameters.

362

## References

- 364 M. J. Betancourt and Mark Girolami. Hamiltonian Monte Carlo for  
Hierarchical Models. *arXiv*, 2013. doi: 10.1201/b18502-5. URL  
366 <http://arxiv.org/abs/1312.0906>.
- Bob Carpenter, Andrew Gelman, Matthew D. Hoffman, Daniel Lee, Ben  
368 Goodrich, Michael Betancourt, Marcus Brubaker, Jiqiang Guo, Peter Li, and  
Allen Riddell. Stan : A Probabilistic Programming Language. *Journal of*  
370 *Statistical Software*, 76(1), 2017. ISSN 1548-7660. doi: 10.18637/jss.v076.i01.  
URL <http://www.jstatsoft.org/v76/i01/>.
- 372 J. J. Egozcue, V. Pawlowsky-Glahn, G. Mateu-Figueras, and C. Barceló-Vidal.  
Isometric Logratio Transformations for Compositional Data Analysis.  
374 *Mathematical Geology*, 35(3):279–300, 2003. ISSN 08828121. doi:  
10.1023/A:1023818214614.
- 376 Jonah Gabry and Tristan Mahr. *bayesplot: Plotting for Bayesian Models*, 2018.  
URL <https://CRAN.R-project.org/package=bayesplot>. R package  
378 version 1.5.0.
- Andrew Gelman and Jennifer Hill. *Data Analysis Using Regression and*  
380 *Multilevel/Hierarchical Models*. Cambridge University Press, Cambridge,  
2006.
- 382 Andrew Gelman, John B Carlin, Hal S Stern, David B Dunson, Aki Vehtari,  
and Donald B Rubin. *Bayesian Data Analysis*. CRC Press, Boca Raton, FL,  
384 3rd edition, 2014.
- By Andrew Gelman, Aleks Jakulin, Maria Grazia Pittau, and Yu-Sung Su. A  
386 weakly informative default prior distribution for logistic and other regression

models. *The Annals of Applied Statistics*, 2(4):1360–1383, 2008. doi:  
388 10.1214/08-AOAS191.

K. Hron, P. Filzmoser, and K. Thompson. Linear regression with compositional  
390 explanatory variables. *Journal of Applied Statistics*, 39(5):1115–1128, 2012.  
ISSN 02664763. doi: 10.1080/02664763.2011.644268.

392 Shanan E. Peters and Michael McClellenn. The Paleobiology Database  
application programming interface. *Paleobiology*, 42(1):1–7, 2015. ISSN  
394 00948373. doi: 10.1017/pab.2015.39.

Shanan E Peters, Jon M Husson, and John J Czaplewski. Macrostrat: a  
396 platform for geological data integration and deep-time Earth crust research.  
*EarthArXiv*, 2018. doi: <http://doi.org/10.17605/OSF.IO/YNAXW>. URL  
398 <https://eartharxiv.org/ynaxw>.

Stan Development Team. Stan Modeling Language Users Guide and Reference  
400 Manual, 2017. URL <http://mc-stan.org>.

K. Gerald van den Boogaart, Raimon Tolosana, and Matevz Bren.  
402 *compositions: Compositional Data Analysis*, 2014. URL  
<https://CRAN.R-project.org/package=compositions>. R package version  
404 1.40-1.